

Jason Baird

Rock Mechanics and Explosives Research Center
University of Missouri-Rolla,
Rolla, MO 65401 USA
telephone: 573-341-6648
e-mail: jbaird@umr.edu

Explosive Shocks and Impedance Mismatch in Armatures¹

Contents

1. Introduction	405
2. Multi-Layered Armatures	408
2.1. Shock Impedance	409
2.2. Experimental Verification	410
3. Summary	410

Abstract

This investigation presents and discusses the influence of impedance mismatch on the explosive expansion of multi-layer armature tubes, as an adjunct to helical flux-compression generator research at the University of Missouri-Rolla, directly affecting the understanding of flux cut-off and high strain-rate changes in generator armatures. A previous investigation, reported elsewhere, studied longitudinal fractures that characteristically developed in single-layer armatures at smaller expansion ratios than predicted by classical analysis. The current study examines shock-produced tensile stresses in the armature skin, and the effects on those tensile stresses caused by density variations within layers of multi-layer armatures. In the original investigation, these tensile stresses produced cracks that occurred within two diameters of the detonator end of the armature, but did not extend when the tubing expanded under explosive pressurization. Such cracks appear to cause magnetic flux cut-off, and flux losses seriously affect energy conversion efficiency. The current study utilizes a two-dimensional Lagrangian finite-difference numerical model, classical impedance-matching calculations, and explosives-loaded multi-layer armature testing to analyze the effect of detonation waves on multi-layer armatures of different compositions. As an extension of the original work, this study further isolates shock wave effects during armature expansion.

1. Introduction

The author is a member of the Explosives Research Group located at the Rock Mechanics and Explosives Research Center (RMERC) of the University of Missouri-Rolla (UMR). In 1998, the Explosives Research Group, along with the Texas Tech University (TTU) Electrical Engineering Department's Pulsed Power Laboratory and researchers from the TTU Mechanical Engineering Department, formed the initial membership of a research consortium whose work has been described elsewhere [1].

Previously published information on explosive-

driven helical flux-compression generator work by the author [2] demonstrated that shock-induced tensile stresses cause cracking in the outer skin of explosively-expanding armatures. The armatures utilized for the testing described in [2] are cylinders made of 6061 aluminum or oxygen-free high-conductivity (OFHC) copper tubing, 3 mm thick and 15 cm long by 3.8 cm in diameter, filled with high explosive. The copper cylinders were annealed to the dead soft state prior to testing, and the aluminum cylinders were tested at both hard and soft states.

High-speed photographs of those single-metal expanding armatures were taken in the detonation tank of the RMERC Explosives Laboratory using a Cordin 010-A framing camera. While examining the armature photographs, the author discovered unusual

This work was primarily funded by the Explosive-Driven Power Generation MURI program funded by the Director of Defense Research & Engineering (DDR&E) and managed by the Air Force Office of Scientific Research (AFOSR).

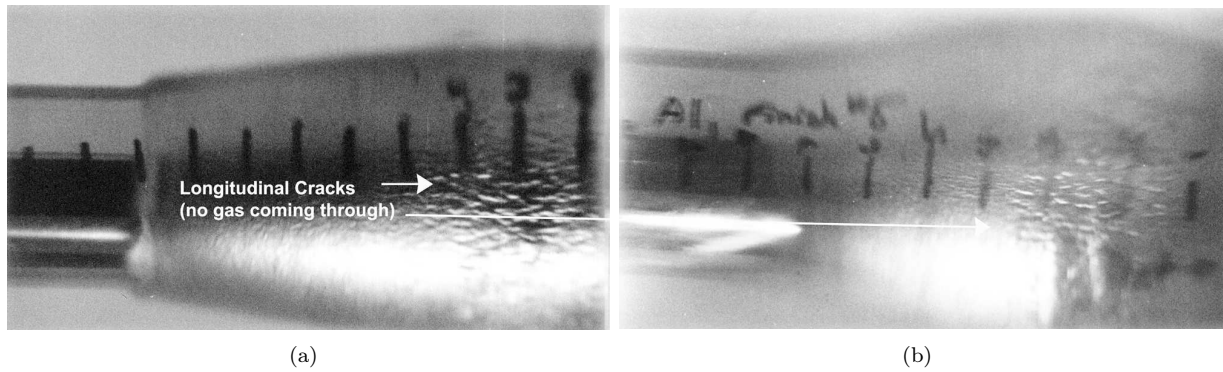


Fig. 1. Armature fracturing. Left – Oxygen-free high-conductivity (OFHC) copper. Right – 6061-T6 Aluminum.



Fig. 2. Cylinder A1 during explosive expansion.

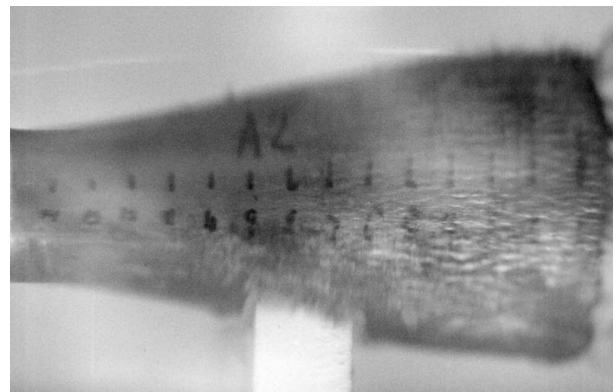


Fig. 3. Cylinder A2 during explosive expansion.

cracking in the armature outer surfaces. The cracks appeared in both metals, no matter which annealed state was used in the tests. In a typical test, as the detonation progressed along the explosive charge the cylinder expanded according to the progress of the detonation through it. The longitudinal cracks, evident on framing camera photographic exposures, began on the surfaces of the detonator end of the cylinders. The cracking was unusual, because in each test, the longitudinal fractures appeared as soon as explosive expansion began, and stopped their extension at identical distances along the cylinders. Fig. 1 is a composite photo of two such cylinders, showing the longitudinal fractures. The fractures were postulated to be the source of one or more generator inefficiencies, due to magnetic flux losses.

The armature is part of the electric circuit within the generator. As magnetic flux within the helical generator is created due to electrical seeding of the stator windings, electric currents begin flowing on the outer surface of the armature in a circumferential direction due to the magnetic field orientation. The flow of these currents must not be disturbed if the flux is to be compressed efficiently between the expanding armature and the stator. If the current flow is disturbed, the magnetic field will be affected. If the current flow is retarded by features such as

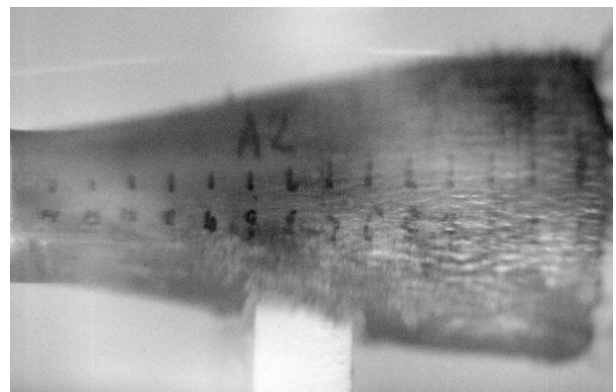


Fig. 4. Cylinder A3 during explosive expansion.

longitudinal cracks on the surface of the armature, it is hypothesized that arcing will occur between the armature and the stator. The arcing will create a very hot plasma, causing the stator insulation to break down before the sliding contact reaches that location. Because arcing causes the current flowing from the armature to the stator to jump ahead of the sliding contact, and the sliding contact is no longer part of the current path, compressed magnetic flux is trapped in the region between the sliding contact and the arc. The trapped flux is lost to the compression process,

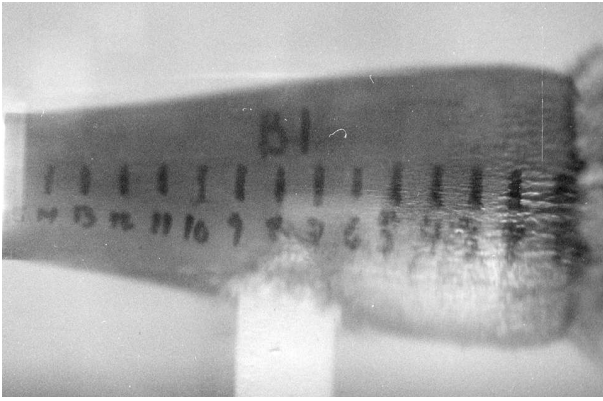


Fig. 5. Cylinder B1 during explosive expansion.



Fig. 7. Cylinder B3 during explosive expansion.

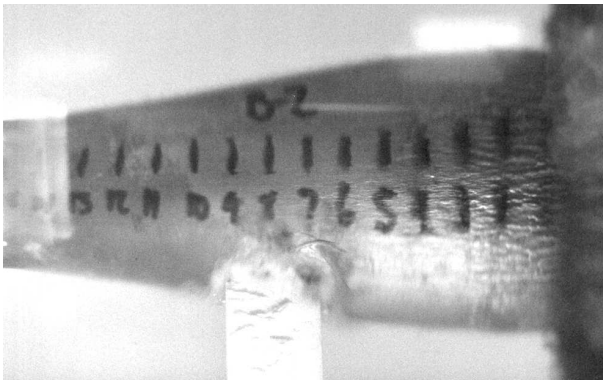


Fig. 6. Cylinder B2 during explosive expansion.

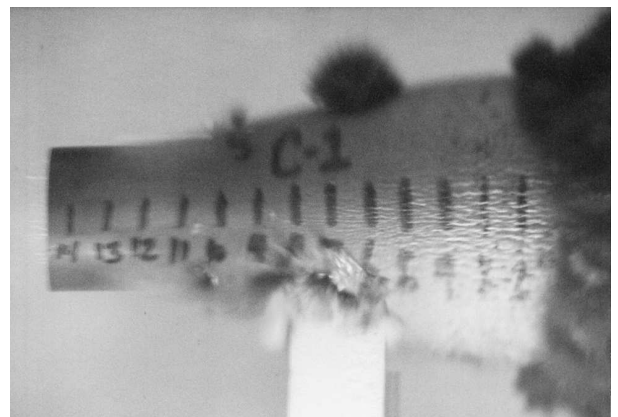


Fig. 8. Cylinder C1 during explosive expansion.

and is a source of inefficiency [3].

In RMERC armature tests, explosive detonation is initiated at the center of one end of the explosive charge within the armature tube. As the detonation wave proceeds through the length of the explosive charge, the armature tube expands into a truncated conical shape and the cone shape moves along the tube in the same direction as the explosive detonation wave. All engineering materials begin to break when stressed beyond their strength limitations, and when the metal in the armature is expanded beyond a certain point it begins to crack. In the armatures tested, this limit is reached when the armature is expanded to about twice its original diameter [4]. Cracking at this degree of expansion would have no effect on generator performance as designed, because the armature has already expanded through the stator and the time for flux compression is completed. In our tests, as expected, after expanding to about two times its original diameter the armature begins to break apart, with high-speed photography showing detonation products escaping through fractures in the metal.

Explosive expansion produces circumferential strains in an armature. Cracks caused by expansion begin where the stresses first exceed the tube material's ultimate strength, and such expansion

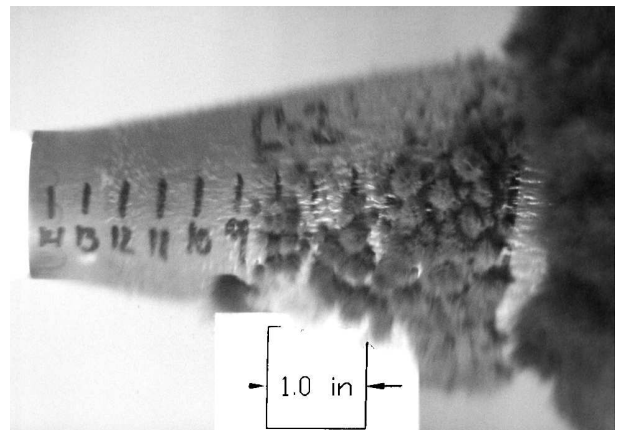


Fig. 9. Cylinder C2 during explosive expansion.

cracks extend from their origins along the armature as the armature is expanded explosively. The fracturing that was the topic of [1] and of this paper, however, occurred much sooner in the expansion process than is expected according to classical stress-strain analysis. As shown by framing camera photography, this longitudinal fracturing only occurs within two diameters of the initiator end of the armatures. Also, after their initiation, the fractures do not extend

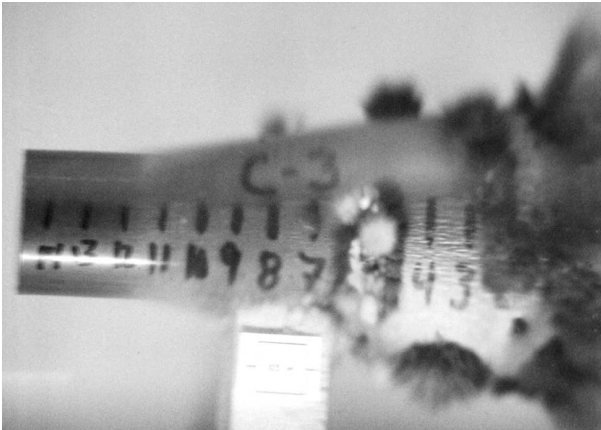


Fig. 10. Cylinder C3 during explosive expansion.

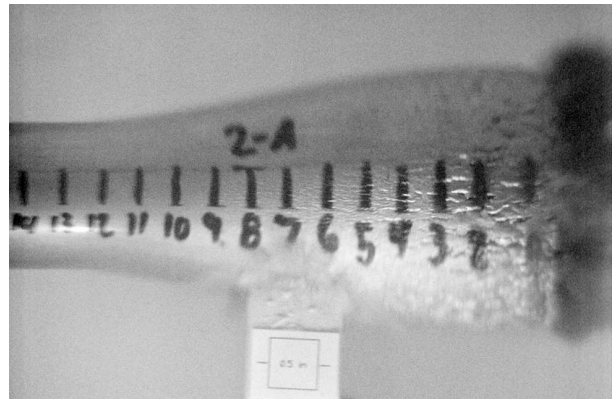


Fig. 12. Cylinder 2A during explosive expansion.

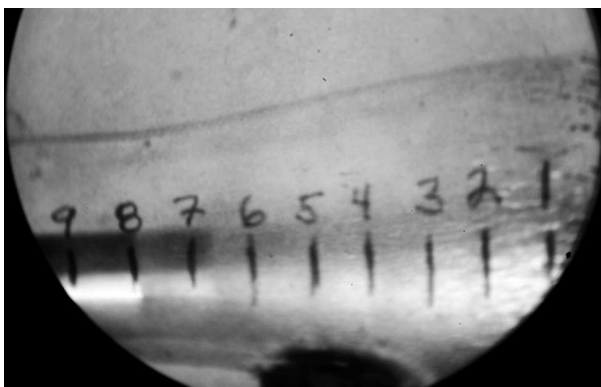


Fig. 11. Cylinder 1A during explosive expansion.



Fig. 13. Cylinder 1B during explosive expansion.

themselves along the expanding tube as would be expected if they were purely a result of explosive expansion of the armatures.

The immediate and easy assumption is that armature expansion is the root cause of the unusual longitudinal fractures. Unfortunately, the fractures occur at much lower armature diameter expansion ratios than was expected in the generator design (< 2). In addition, classical analysis shows that explosive expansion causes cracks that begin on the inner surface of the armature, but the longitudinal cracks noted in our high-speed photos began on or near the outer surface. These were two of several clues lead to suspicion that shock dynamics, rather than explosive pressurization, is the root cause of the fracturing [1].

Given the alternating compressive and tensile stresses in the first two diameters of end-initiated armatures, as predicted by analysis and simulation [1], it is reasonable to expect that longitudinal cracks form where tensile detonation wave reflections occur as shocks traverse the large density change from armature metal to the surrounding atmosphere. These tensile waves cause crack initiation points. The points form a preconditioned, damaged area through low-cycle fatigue. Immediately after the crack initiation loci are created, compressive stresses are

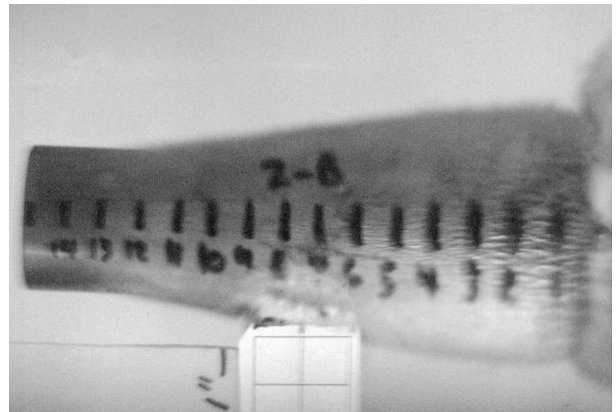


Fig. 14. Cylinder 2B during explosive expansion.

imposed on them, keeping the incipient cracks closed. These incipient flaws are opened into cracks a few microseconds later, as expansion of the armature tube due to explosive pressurization begins. The regions farther down the tube, beyond the preconditioned area, expand normally and do not crack until the tube expands beyond the stator position.

2. Multi-Layered Armatures

When a shock wave moving through a medium



Fig. 15. Cylinder Lex 1 during explosive expansion.

arrives at a boundary, it may partially or totally reflect back into the incident medium as a compressive wave or as a rarefaction, or it may be entirely transmitted into the adjoining medium. What happens to the wave depends on the degree of shock impedance mismatch between the media at the boundary.

2.1. Shock Impedance

The shock impedance of a material is equal to the product of its pre-shocked density and the velocity of the shock in the material. When it impinges on a boundary, the shock wave will reflect as a compressive wave if the adjoining medium has higher shock impedance than the incident medium or as a rarefaction (tensile wave if in a solid) if the adjoining medium has lower shock impedance than the incident medium. No reflection will take place if the impedances are equal. The greater the impedance mismatch, the greater the portion of the shock energy reflected, and the smaller the portion transmitted. This has been verified experimentally [5].

The author postulated that including low-density layers between high-density materials through the thickness of the armature would affect the tensile stress generated within the outer layer by reflection of the shock as it leaves the armature. Each reflection should reduce the shock energy transmitted to the next material layer. To verify this, simulations were performed of a multi-layer armature, composed of inner and outer 1 mm layers of OFHC copper with a 1 mm inner layer of acrylic polymer (Plexiglas®), using the Two-Dimensional Lagrangian code (TDL) from [6]. The simulation investigated tensile stress reduction in the outer, metal layer through impedance mismatch within the armature thickness. The simulation predicted lower tensile stresses at the armature surface than in metallic armatures, but the stresses still exceeded the ultimate strength of the copper outer layer. Additionally, the region of tensile stress in the simulation spans most of the outer layer, and it moves along the length of the armature as the simulation progresses. This is in contrast to the single layer armature, wherein the

tensile stress region follows a trajectory away from the armature surface after its initial appearance.

As another check of this postulate, shock impedances were calculated and the expected outcome of testing based on those results was compared to actual test results generated by explosive testing of multi-layer armatures.

The shock impedances of the materials involved in the testing were determined in the following manner [5,7].

Determination of the pressure and particle velocity at a material interface allows calculation of shock impedance:

$$\begin{aligned} Z &= \rho_0 U, \\ P &= \rho_0 u U, \\ Z &= \rho_0 \left(\frac{P}{\rho_0 u} \right) = \frac{P}{u} \end{aligned} \quad (1)$$

where Z is shock impedance, ρ_0 is initial density, u is interface particle velocity, U is shock velocity, and P is interface pressure. Note that in this set of calculations:

- Shock pressure at the explosive charge to armature interface was determined to be 38.65 GPa [8].
- The detonation/shock wave travels from left to right across the material interface.

The governing Hugoniot equation for waves traveling from left to right is:

$$P = \rho_0 C_0 u + \rho_0 S u^2. \quad (2)$$

(2) The governing Hugoniot equation for waves traveling from right to left is:

$$P = \rho_0 C_0 (u_0 - u) + \rho_0 S (u_0 - u)^2 \quad (3)$$

C_0 and S are unreacted Hugoniot coefficients, and along with the initial density, they were determined to be:

	ρ_0 , g/cm ³	C_0 , km/sec	S
acrylic (Lucite®/ Plexiglas®) [7]:	1.181	2/260	1.816
6061 Aluminum [9]:	2.703	5.350	1.340
OFHC Copper [7]:	8.930	3.940	1.489
Atmosphere (air, helium, etc.) [7]	0.001	0.899	0.939

The technique used to generate the impedances is to work from the known shock pressure at the inner surface of the armature, outward through the armature layers and their interfaces, calculating unknowns and using them in (2) and (3) to find

interface pressures and particle velocities. These pressures and velocities are then used in (1) to find the shock impedance between the two layers.

First, the particle velocity in the innermost layer of the armature (the material next to the explosive charge) is found using the explosive shock pressure in (2), the right-traveling wave equation. Substituting the derived particle velocity and the explosive shock pressure into (1) produces the impedance at the explosive-innermost layer interface. Next, since the pressures within the innermost layer and the next (second) layer are equal at their interface, the equation of the (left-traveling) wave reflected from the interface (3) is set equal to the equation of the (right-traveling) wave transmitted through the interface (2) and the combined equation solved for the particle velocity at the interface. Using the resulting value for particle velocity in the second layer, (2) is solved for the shock pressure within the second layer. As before, use of the particle velocity and the shock pressure in equation (1) produces the shock impedance at the second interface.

This procedure, when utilized in a step-wise fashion through the thickness of the armature, gives the shock impedances for each layer of the armature, and for the atmosphere surrounding the armature. Comparison of the final two impedances determines the impedance mismatch seen by the shock as it leaves the armature. As a figure of merit, the smaller the absolute value of the impedance mismatch, the less shock energy reflected back into the armature material, and the lower the tensile stress generated within the outer layer of the armature.

Examination of the results (Table 1) indicates that an armature with copper inside and aluminum outside has the lowest impedance mismatch, followed closely by a simple, single-layer aluminum armature. Impedance mismatch results are in step with the simulation results. Including an acrylic layer or an atmosphere layer within the thickness of the armature produces no apparent advantage.

2.2. Experimental Verification

To verify the simulation and impedance mismatch results, multi-layer cylinders were tested. For these tests, two different photography methods were used. High-speed Cordin framing camera photography (1 frame per 2 μ sec) was used to take the photos of the A, B, C, 2A, 2B, and Lex 1 cylinder tests, while a digital camera was used to photograph the 1A and 1B tests. The digital images were acquired using a gated image intensifier that allowed single frames to be taken with an exposure of 60 nanosec per frame.

The "A" and "B" series of tests utilized bi-metallic cylinders having copper outside and aluminum inside; the "A" series with the aluminum approximately twice the copper thickness, and the "B" series of tests

having the copper approximately twice the aluminum thickness.

The "C" test series utilized multi-layered cylinders composed of layers of copper (outside), Flexaner rubber (middle), and aluminum (inside). The cylinders in these tests were each 15 cm long, 3.8 cm outside diameter, with consistent thicknesses for each cylinder that varied from 2.82 to 3.43 mm (Table 2).

The primary observation made from this data indicates that expansion angle is sensitive to armature density; generally, the armatures with aluminum in greater proportion of the total thickness demonstrate greater expansion angle compared to those with a greater proportion in copper. The "C" series cylinders approached the performance of the "A" series, according to this data.

Unfortunately, the data do not reflect the appearances of the armature surfaces during explosive expansion. Figures 2 through 10 contain photos of each of the cylinders in the three series, with each photo taken at approximately the same point in explosive expansion. Note that the surfaces of the "B" series cylinders are smoother, beyond about 4 cm from the initiation end of the explosive charge, than those of the "A" series. The "C" series cylinders did not perform to expectations. Apparently, voids within the cured Flexane® material caused rapid, almost random penetrations of the outer, copper layer of each cylinder during explosive expansion. Depending on the method of assembly, it is very difficult to form a void-free layer between cylindrical metal layers when using an in-situ cured elastomer such as Flexane® as the filler.

Figures 11 through 15 contain photos of cylinders 1A, 2A, 1B, 2B, and Lex 1 (aluminum with an inner liner of Lexan® plastic) undergoing explosive expansion, with the digital photos (1A and 1B) taken earlier in the expansion process than the film photos. The external surfaces are smoother and cracking is less severe in the cylinders with aluminum outer layers (1A, 2A, and Lex 1) than in the cylinders with copper outer layers (1B and 2B). The expansion performance of these cylinders parallels that of the "A" and "B" series cylinders as mentioned above.

3. Summary

The postulate that premature longitudinal cracking in armatures could be controlled by forcing shocks and rarefactions to transit surfaces between materials of large density difference was not verified in this series of simulations, analyses, and tests. Armatures composed of an inner OFHC copper layer and an outer layer of 6061 aluminum had lower impedance mismatches at their outer surfaces than all other designs; their superiority, however, was not large enough,

Table 1. Multi-layered armature material impedance matching

	P at material to C-4 interface= 38.65					At first cylinder material interface			At interface at outer surface of cylinder		
		ρ_0 , g/cm ³	Inner material			Inter- face	Impedance		Inter- face	Impedance	
			Unreacted Hugoniot coefficients	Impe- dance	P		Outer material	Diffe- rence		Outer material	Diffe- rence
		C, km/sec	S	Z	P	Z	Z _{diff}	P	Z	Z _{diff}	
Explosive-Acrylic-Aluminum-Atmos	Acrylic-Aluminum-Atmosphere	1.181 2.703 0.001	2.260 5.350 0.899	1.816 1.340 0.939	10.536	98.043	27.414	16.878	0.070	0.010	-27.405
Explosive-Aluminum-Copper-Atmos	Aluminum-OFHC copper-Atmosphere	2.703 8.930 0.001	5.350 3.940 0.899	1.340 1.489 0.939	21.097	74.535	53.655	32.559	0.013	0.005	-53.651
Explosive-Copper-Aluminum-Atmos	Aluminum-OFHC copper-Atmosphere	2.703 8.930 0.001	5.350 3.940 0.899	1.340 1.489 0.939	46.287	25.611	19.274	-27.013	0.012	0.004	-19.270
Explosive-Atmos-Copper-Atmos	OFHC copper-Atmosphere	8.930 0.001	3.940 0.899	1.489 0.939	0.217	154.177	66.167	65.950	0.032	0.007	-66.160
Explosive-Atmos-Aluminum-Atmos	Aluminum-Atmosphere	2.703 0.001	5.350 0.899	1.340 0.939	0.217	154.152	31.941	31.724	0.124	0.013	-31.928
Explosive-Aluminum-Atmos	Aluminum-Atmosphere	2.703 0.001	5.350 0.899	1.340 0.939	21.097				0.021	0.006	-21.091
Explosive-Copper-Atmos	OFHC copper-Atmosphere	8.930 0.001	3.940 0.899	1.489 0.939	46.287				0.005	0.003	-46.284

All P are in GPa

Table 2. Multi-layered armature test results

Cylinder	Layer Thickness, mm				Expansion	
	Outside	Middle	Inner	Total	Ratio	Angle, deg.
	Copper	Flexane®	Aluminum			
A1	1.14	n/a	2.29	3.43	1.9	12.0
A2	1.27	n/a	2.01	3.28	2.2	13.0
A3	0.86	n/a	2.16	3.02	2.2	12.5
Average	1.09		2.15	3.24	2.1	12.5
B1	1.91	n/a	1.27	3.18	1.8	9.0
B2	2.03	n/a	1.02	3.05	2.0	12.0
B3	1.98	n/a	1.19	3.17	1.8	8.5
Average	1.97		1.16	3.13	1.9	9.8
C1	1.14	0.91	1.14	3.19	2.0	14.0
C2	1.12	0.97	1.24	3.33	2.0	11.5
C3	0.89	0.89	1.04	2.82	1.9	11.5
Average	1.05	0.92	1.14	3.11	2.0	12.3
	Aluminum		Copper			
1A	(not measured)	n/a	(not measured)		1.6	11.0
2A	1.56	n/a	1.56	3.12	1.7	12.0
Average					1.7	11.5
1B	(not measured)	n/a	(not measured)		1.5	10.0
2B	1.61	n/a	1.55	3.16	1.9	10.0
Average					1.7	10.0
	Aluminum		Lexan®			
Lex 1	3	n/a	3.18	6.18	2.0	13.0

compared to single layer armatures of 6061 aluminum, to make their extra complexity worthwhile. The simulations and analyses were verified by high-speed framing photography.

It is possible that further layering, or use of other metals combined with less dense materials, will reduce tensile strains in the outer armature skin to the point that premature cracking will not occur. Unfortunately, the contract under which this work is being performed will end shortly, and not further funding is anticipated.

Acknowledgement

The author would like to acknowledge the assistance of Dr. Jahan Rasty of Texas Tech University, for providing some of the materials used in testing.

Manuscript received October 10, 2003

References

- [1] Baird J. and Worsley P.N. The Causes of Armature Surface Fracturing Within Helical Flux Compression Generators // IEEE Trans. on Plasma Sci. Sp. Issue on Pulsed-Power Sci. and Tech. – Oct. 2002. – V. 30, N. 5. – P. 1647–1653.
- [2] Neuber A.A., Dickens J.C., Krompholz H., Schmidt M.F.C., Baird J., Worsley P.N., and Kristiansen M. Optical Diagnostics on Helical Flux Compression Generators // IEEE Trans. Plasma Sci. – Oct. 2000. – V. 28, N. 5. – P. 1445–1450.
- [3] Knoepfel H.E. Pulsed High Magnetic Fields. – Amsterdam: North-Holland. – 1970.
- [4] Ugural A.C. and Fenster S.K. Advanced Strength and Applied Elasticity. – New York: Elsevier North Holland. – 1979.

- [5] Cook M.A. The Science of Industrial Explosives.
– Salt Lake City, Utah: IRECO Chemicals.
– 1974.
- [6] Mader C.L. Numerical Modeling of Explosives
and Propellants, Second Edition. – New York:
CRC Press. – 1998.
- [7] Cooper P.W. Explosives Engineering. – New
York: Wiley-VCH. – 1996.
- [8] Shkuratov S.I., Talantsev E.F., Dickens J.C.,
Kristiansen M., and Baird J. Longitudinal-
Shock-Wave Compression of Nd₂Fe₁₄B High-
Energy Hard Ferromagnet: The Pressure-Induced
Magnetic Phase Transition // Applied Physics
Letters. – Feb. 2003. – V. 82, No. 8. – P. 1248–
1250.
- [9] Marsh S.P., ed. "LASL Shock Hugoniot
Data," Los Alamos Series on Dynamic Material
Properties. – Berkeley: University of California
Press.
– 1980. – P. 182.